

Article

A Framework for Characterizing Flapping Wing Systems

Alex T. Lefik^{1,*}, Romeo M. Marian¹, Titilayo Ogunwa¹ and Javaan S. Chahl^{1,2}¹ UniSA STEM, University of South Australia, Mawson Lakes, SA 5095, Australia² Joint and Operations Analysis Division, Defence Science and Technology Group, Melbourne, VIC 3207, Australia

* Correspondence: alex.lefik@mymail.unisa.edu.au

Abstract: Flapping wing systems are being developed by various institutions and research groups around the world with many systems developed that are capable of full flight. However, while instrumentation has been developed that is capable of measuring some of the characteristics of these systems, there is no complete solution. This paper seeks to take the first step toward instrumentation that could be applied to any flapping wing system. This first step is to identify and characterize the forces that are operating on flapping wing systems. This paper presents, in premiere, a systematic analysis of all cases that can create useful or parasitic aerodynamic loads along with the other major loads that would be experienced by these cases and methodology for how these can be measured with the ambition that it can become a framework to be used to characterize any flapping wing system.

Keywords: instrumentation; UAVs; sensing; flapping; dynamics; biomimetics



Citation: Lefik, A.T.; Marian, R.M.; Ogunwa, T.; Chahl, J.S. A Framework for Characterizing Flapping Wing Systems. *Drones* **2022**, *6*, 398. <https://doi.org/10.3390/drones6120398>

Academic Editors: Bo Cheng and Mostafa Hassanalian

Received: 19 October 2022

Accepted: 30 November 2022

Published: 6 December 2022

Publisher's Note: MDPI stays neutral with regard to jurisdictional claims in published maps and institutional affiliations.



Copyright: © 2022 by the authors. Licensee MDPI, Basel, Switzerland. This article is an open access article distributed under the terms and conditions of the Creative Commons Attribution (CC BY) license (<https://creativecommons.org/licenses/by/4.0/>).

1. Introduction

Flapping wing unmanned aerial vehicles (UAVs) are a potential solution to the limited flight envelopes of existing fixed and rotary wing UAVs. Current systems are generally restricted to either high-speed forward flight, requiring a runway to take off or land (fixed wing) [1,2], or low-speed flight capable of hover and vertical take off and landing (VTOL), but these are inefficient over extended distances (rotary wing) [3]. Systems in nature are capable of performing both low-speed and hovering manoeuvres, as well as high-speed, efficient flight in a single system.

One example of a system with these performance characteristics is the dragonfly. They are capable of forward velocities as high as 10 ms^{-1} and instantaneous accelerations of 25 ms^{-2} for the first 0.1 s of flight [4]. They are also efficient, being able to travel up to 20.8 cm per wing beat [4], achieve lift to drag ratios approaching 10:1 [5,6] and documented cruising migration ranges of up to 800 km [7].

Moreover, they are capable of rolling their bodies like a fixed wing craft at up to 180 deg/s in two to three wing beats and yawing as quickly as 180 deg within three wing beats [8].

This shows that these natural systems are capable of achieving performance similar to both fixed and rotary wing craft, with speed, efficiency and maneuverability.

Due to the potential to bridge this performance gap, flapping wing systems are being developed by a variety of institutions and research groups around the world; however, no system has come close to emulating the impressive performance characteristics of natural flyers.

A significant deficiency in these developmental flying systems has been their lack of instrumentation. This probably prevents design improvements and also prevents online control of the wings. Instrumentation is also vitally important for flapping wing systems in particular as their low mass and high complexity make it imperative to fully measure performance. This would enable deficiencies to be located and rectified, increasing the overall efficiency of the system. To further highlight the importance of instrumentation in

flapping wing systems, the level of sensing present in natural systems is incredibly detailed to be able to handle the flight requirements. Birds have been shown to have sensory receptors in their feathers [9–12] to detect changes in airflow and air current allowing them to react accordingly during flight. Compared to this level of sensing, current man-made flapping wing systems suffer a major disadvantage.

To deeper investigate this deficiency, many different flapping wing systems were assessed to determine what methods of instrumentation were used. These types of instrumentation, along with what aspects of system performance they are capable of measuring, are shown in Table 1. This shows both the use cases and deficiencies of each method and how much of the complete system can be characterized by each.

Table 1. Existing Instrumentation.

Instrumentation	Mech In	Wing In	Wing Aero/Inert	Total Force
Bench mount force sensor [13–34]	No	No	No	Yes
Wind tunnel and force sensor [35–39]	No	No	Yes *	Yes
Load cell attached to wing root and vacuum vessel [40,41]	No	No	Yes	Yes
Motor torque profiles [42]	Yes	No	No	No
Counterbalance beam with angle sensor [43]	No	No	No	Calculated

The instruments in Table 1 do not include systems that utilized simulation models or calculations. While these are useful in understanding the performance of a system, they cannot be used to provide real-time data during system performance, which is essential to creating a fully optimized flapping wing system. They also only include force measuring instrumentation, not instrumentation measuring the kinematics, although this is also important.

Here:

- Instrumentation: The type of instrumentation.
- Mech In: Does the instrumentation measure the loading input to the mechanism?
- Wing In: Does the instrumentation measure the loading input to the wing?
- Wing Aero/Inert: Is the instrumentation capable of characterizing the wing loading as aerodynamic or inertial?
- Total Force: Can the instrumentation measure the total force output by the system?

The first type of instrumentation and by far the most common is to use a force sensor attached to the system in a bench test. The mounting points can vary between systems, with some mounted on the wing and others mounted to the base of the wing, but the most common method is to mount the entire system on the sensor itself.

The sensors also vary in these systems, with some using a single axis load cell/force sensors and others using multi-axis load cells. The main difference between these methods is that any system measured on a single axis load cell needs to be reoriented between tests to allow the sensor to measure forces upon the different axes during system operation.

These systems are relatively simple to set up and can offer accurate measurements using well-known and understood sensors. They can also give an indication of whether there are improvements in the overall force generated by the system between tests.

However, there is a lot of information the sensor is not able to capture regarding the system's performance as can be seen from Table 1. This type of instrumentation does not examine any of the performance of the motor or mechanism leading into the wing, meaning there is potential for unidentified energy losses in the system. The instrumentation also does not offer any way to determine the inertial load created by the wing so that it can be separated from the aerodynamic load.

Overall, this method of instrumenting flapping wing systems is feasible for determining changes to a system's overall performance as the system is being developed, but it does not offer the full picture of system performance that would be required for characterization and certainly does not allow online use during operation.

The second method of instrumentation is using a force sensor in a wind tunnel. This still suffers most of the same deficiencies as using a force sensor on a bench with it lacking readings on where losses might be occurring prior to transmission to the wing itself in the system.

The advantage that wind tunnel testing has is that it can give insight into the performance of each wing in an air stream along with how air flow over the wing will impact on performance while the system is in operation. However, it lacks any means to separate the aerodynamic and inertial loading that is caused by flapping (separate to the airflow), which is necessary to ensure as much of the energy as possible is being put into useful loading and not lost to inertia, hence the asterisk in Table 1.

The next method of instrumentation is to combine a load cell attached to the wing root with testing in a vacuum chamber. The immediate advantage to this method is that it enables the aerodynamic and inertial loading to be isolated from each other. This means the energy being lost to inertia can be fully understood, which allows further characterization of the wing's performance.

The main disadvantage to this form of measurement is that it is unable to provide any measurements of the system prior to the wing. This means that if there is a complex mechanism/gearbox where losses could be incurred, this system cannot detect any potential issues.

Another method of instrumentation is utilizing the torque profiles of a motor during its operation. This gives a clear insight into what forces are being input into the mechanism to be transmitted to the wing, which is useful information when trying to determine the efficiency of the system.

The disadvantage of this type of measurement is clear, it does not give any insight into the lift performance of the system itself. However, this measurement is best utilized in tandem with other instrumentation further along in the system to cross-check and validate performance, so this deficiency is not a major issue.

The final method of instrumentation has been a counterbalanced beam. This method has the flapping wing system mounted to one end of a beam and a counterbalance attached to the other. The measurements are obtained using an angle sensor, and the calculation of the force generated by the system utilizes this value.

Such systems have similar deficiencies to the bench tests using force sensors in that they do not characterize the performance of the mechanism upstream of the wing nor does it characterize the full performance of the wing itself. This system also appears to be a more complex solution to the bench top force measuring system without offering any significant advantages.

Overall, it can be seen that there is no type of instrumentation that is capable of measuring the full system performance of a flapping wing system from the motor/actuator through to the forces released from the wing. It is still necessary to determine instrumentation or a testing regime that can satisfy all of these requirements, which will potentially require multiple sensors reading in multiple locations to provide the full necessary data.

When concept instrumentation was built in order to check the validity of smaller sensors that could potentially be put into more useful locations on a flapping wing system, it seemed to demonstrate that there is potential for force sensing resistors to be used to understand the forces acting on the system during operation [30].

For a full instrumentation suite to be designed, it is necessary to understand exactly what needs to be measured and where these measurements need to take place. This has the capability of discriminating different types of forces and unraveling the complexity of the flapping wing system.

In the case of flapping wing UAVs, this is particularly necessary as the complexity of the system means there are many sources of potential losses that could rapidly cripple a system's performance if they are not identified, minimized and managed. Once a system's losses and performance characteristics are properly understood, the requirements for exactly what needs to be measured and where these measurements need to take place becomes clearer, and instrumentation that will suit the system can be properly designed.

Table 2 shows the nomenclature used for the remainder of this paper.

Table 2. Nomenclature.

Symbol	Meaning	Units
\vec{F}_w	Net force on wing	N
F_{wx}, F_{wy} and F_{wz}	Forces on wing in x, y and z directions	N
\vec{i}, \vec{j} and \vec{k}	Unit vectors of wing coordinate system	-
$\vec{F}_{xi}, \vec{F}_{yi}$ and \vec{F}_{zi}	Forces acting on body from wing i	N
$\vec{M}_{pi}, \vec{M}_{qi}$ and \vec{M}_{ri}	Moments acting on body from wing i	N·m
T_w	Torque input to wing	N·m
T_a	Torque input to mechanism	N·m
η_m	Mechanical efficiency of mechanism	-
F	Force applied to mechanism joint	N
$\theta_w, \dot{\theta}_w$ and $\ddot{\theta}_w$	Flapping angular position, velocity and acceleration of wing	rad, rad s ⁻¹ , rad s ⁻²
β	Pitching angle of wing (about lift axis)	rad
γ	Lead lag angle of wing (perpendicular to θ)	rad
t	Time	s
T_I	Torque loading due to inertia	N·m
I_w	Wing moment of inertia	kg·m ²
r	Wing sectional radius	m
m	Wing sectional mass	kg
V_∞	Air velocity over wing	ms ⁻¹
V_w	Wing velocity caused by motion of wing	ms ⁻¹
L, D	Lift and drag	N
L_w and D_w	Lift and drag in wing reference plane	N
L_b and D_b	Lift and drag in body reference plane	N
C_L and C_D	Coefficients of lift and drag	-
ρ	Air density	kg/m ³
A	Wing area	m ²
R	Total length of wing	m
V_{wr}	Velocity from wing motion acting upon section radius r	ms ⁻¹
A_{wr}	Area of wing at section radius r exposed to velocity V_{wr}	m ²
A_∞	Area of wing exposed to air velocity V_∞	m ²

2. Dynamics

Due to their distinctly different morphology to traditional aircraft, flapping wing systems have different dynamics to consider when analyzing the forces acting on them.

The first difference in comparison to traditional aircraft is how the forces are generated. In a fixed or rotary winged aircraft, the force is generated by an airfoil moving through the air and generating both aerodynamic lift and drag relative to its velocity.

A flapping wing system generates forces in two distinct ways simultaneously. The first is in a similar fashion to a fixed wing aircraft—with the velocity of air over the wings generating lift and drag forces. The second is significantly more complex as it is forces that are generated by the wing's motion through the air relative to the body. This is more analogous to a rotary winged aircraft; however, the movement is oscillatory and potentially of arbitrary form rather than rotational. The measurement of either of these forces is complex due to the constant changing of a wing's exposed surface area to either the velocity of the air caused by the craft's movement or the relative velocity of the air caused by the wing's movement.

There is also the added complexity of the wings on a flapping wing craft being flexible. This means that the force being generated by the flapping of the wing, which is at least of the order of magnitude of the conventional aerodynamic lift generated, is out of phase with the motion of the wing itself, as the tip of the wing would be lagging behind the root of the wing during the acceleration phase of oscillatory motion and can lead the root wing during deceleration.

The second difference is the force transfer from the wings to the craft. In a fixed wing aircraft, the wings and the body are all functionally rigid during operation such that the loading from the wings is directly transferred into the body of the aircraft. Any flexibility in the system is negligible in a fixed wing aircraft.

In a flapping wing system, however, the wings are constantly moving relative to the body, with multiple degrees of freedom. This means that the resultant force from each wing is constantly changing direction while the wing is actuating and leads to added complexity when attempting to operate a flapping wing system with two or four wings as the forces from each wing have to be used in tandem to generate the desired motion; otherwise, there is a chance of undesirable movement in any direction which is wasted energy.

This necessitates being able to transform the forces acting upon the wing's coordinate frame to that of the body's coordinate frame to be able to determine the net forces acting upon the craft. To start with, every force acting on the wings (all of which are explained in more detail in Section 3) will generate loading that does not conform to a single axis; as such, the three directional forces on each wing can be expressed along the three axes to yield F_{wx} , F_{wy} and F_{wz} , respectively. Adding these vectors would yield the net force for a particular wing.

$$\vec{F}_w = F_{wx}\vec{i} + F_{wy}\vec{j} + F_{wz}\vec{k} \quad (1)$$

where \vec{i} , \vec{j} and \vec{k} represent the unit vectors of the wing coordinate system.

While this provides the forces in terms of the wing coordinate system, the wing is constantly moving relative to the body, meaning this coordinate system is not suitable and would need to be converted to the coordinate system of the body.

These forces when converted would yield forces acting in the direction of the body of the craft's three primary axes, akin to fixed wing aircraft. These forces generated by a specific wing i would be \vec{F}_{xi} , \vec{F}_{yi} and \vec{F}_{zi} .

Due to these forces not occurring at the center of mass of the craft, the moments generated by them also need to be considered. These moments are determined using the forces acting upon each axis and the axial distance between the wing (where the force is acting) and the center of mass and are represented by M_{pi} (about x axis—roll), M_{qi} (about y axis—pitch) and M_{ri} (about z axis—yaw) for wing i .

By summing all of the forces and moments acting on common planes, the net force along each of the three axes of the body plane (\vec{F}_x , \vec{F}_y and \vec{F}_z) along with the net moments about each primary axis (M_p , M_q and M_r) can be determined. These net forces will be what ultimately generates the craft's movement during operation.

This shows that even when the forces acting upon each wing are known, there is still an added layer of complexity in flapping wing systems in order to fully characterize how the loading is impacting system performance.

3. Analysis

The total force in the actuation–support–wing system, besides the weight of the craft, is a combination of the following distinct forces:

- Friction;
- Inertial Loading;
- Aerodynamic Loading;
- Elasticity.

These forces, which have been demonstrated to be reliably measurable, are analyzed in more detail in the next section except for elasticity, which is beyond the scope of this paper. Additionally, the next section shows the sequence in which these measurements need to be taken so the correct contribution of each individual force can be determined.

This sequencing of the testing is important because it enables the components of the system performance that are more straightforward to be characterized first, before using this understanding in the determination of the more challenging variables.

Table 3 shows the separation of these variables in the proposed sequencing of tests. As the table shows, working through this sequence enables each of the variables to be separated, fully quantified and measured before variables with more complex expressions are introduced back into the system.

Table 3. Forces in Test Sequence.

	Forces Present			
	Friction	Inertia	Aerodynamics	Elasticity
No Wing	X			
In Vacuum	X	X		
Rigid Wing	X	X	X	
Normal Wing	X	X	X	X

The following sections detail what these tests would entail in regard to the methodology and apparatus. The apparatus are representative to suit the testing methodology and would be capable of utilizing different inputs (actuators) or outputs (wings) to test a variety of system components. The sensing itself is designed in to be minimally invasive to system and compact enough to be integrated into space-restricted systems.

This is with the anticipation that a similar testing methodology can be utilized by any existing system or any new system designed.

3.1. Friction

The first of the forces to consider during the operation of the flapping wing is friction. Any loading due to friction is detrimental to the system as friction is loss, and there is no way to convert it back into useful energy. Friction energy is dissipated as heat in the environment.

It is therefore necessary to be able to categorize the friction in the system as a precursor step before attempting to minimize it as much as possible.

Figure 1 shows the parameters that need to be measured/considered in order to determine the frictional loading in the wing joint. T_w is the actual torque that is experienced by the wing, while T_a is the torque being applied into the system. As the amount of frictional loss directly impacts the efficiency of the system, these can all be determined using the following equations in which η_m represents the mechanical efficiency of the mechanism.

$$T_w = \eta_m T_a(t) \quad (2)$$

When the system is only operating in one plane, this relationship adequately represents the efficiency of the mechanism with respect to the frictional loading. As more degrees of freedom are added, the complexity of the motion increases. This would be reworked to represent the loading in all planes/axes instead of just one.

The efficiency of the joint depends on a number of factors:

$$\eta_m = f(F, \theta_w, \dot{\theta}_w) \quad (3)$$

where:

- F —the force applied to the joint;
- θ_w —the angular position of the wing;
- $\dot{\theta}_w$ —the angular velocity of the wing.

All three variables need to be measured or controlled.

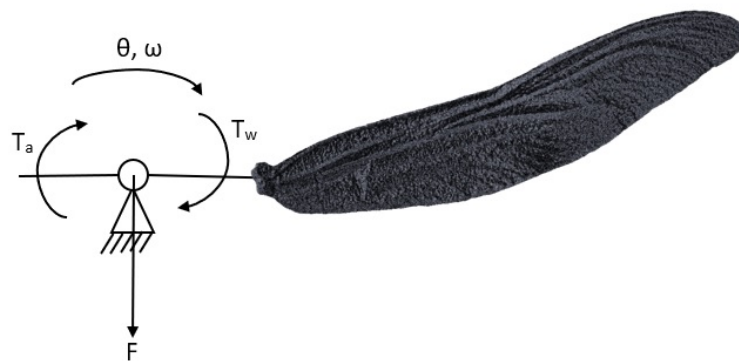


Figure 1. Frictional Loading on the Wing (wing model source: [44–46]).

This would permit the understanding of the performance of the mechanism. Due to the mechanism's characteristics being independent to those of the wing itself, this testing would be carried out first in the determination of a system's performance. A testing apparatus that could be used for this purpose is shown in Figure 2.

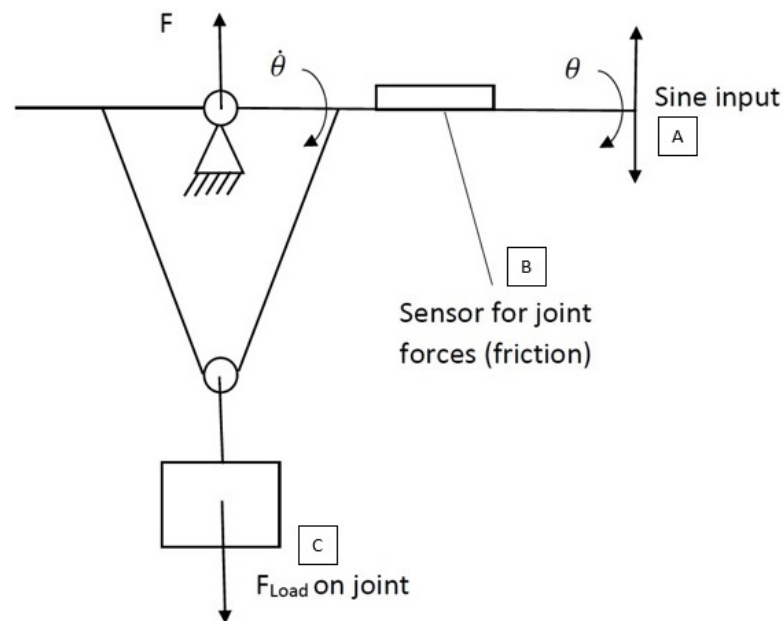


Figure 2. Friction Testing Setup.

This mechanism comprises several parts. The first of these is the core of a flapping wing system, featuring the lever arm and the pivot point for the root of the wing but not including the wing itself. This is to isolate the joint, so the frictional loading is the only force acting upon it (bar other forces which are effectively negligible).

The second component is a motion generator (A). This would be a mechanism to generate a sine output in the same manner as mechanism 1283 from Volume 2 of Artobolevsky's design handbook [47]. An example system is shown in Figure 3.

The next component is the loading, which is distributed across either side of the joint (C). This loading can be achieved either using masses or through direct application of force as long as the magnitude is accurately quantifiable and controllable. This loading is what will generate the friction force in the joint that the testing apparatus will be measuring. It is imperative that the measurement system does not add to the complexity.

The final component of the system is the sensor itself (B) which will measure the bending force. This will then be translated as the friction force. This sensor will be applied

to the lever arm of the wing and will measure the loading on the wing during the operation of the test.

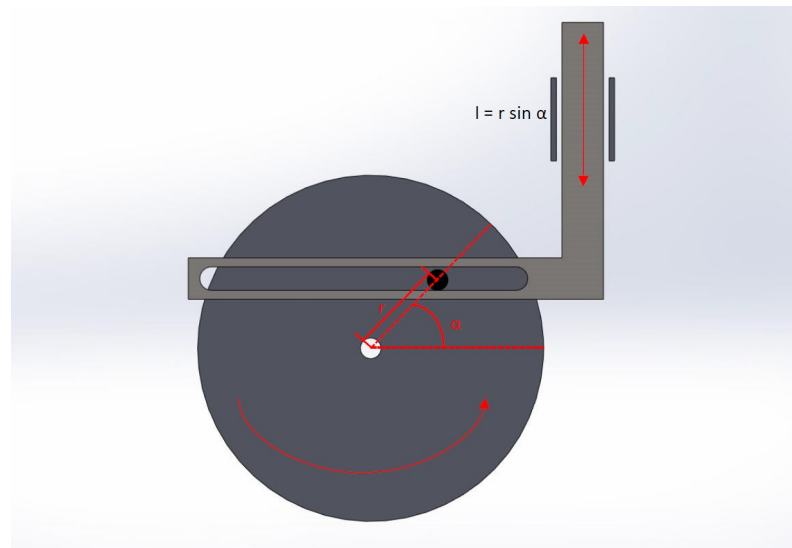


Figure 3. Example of a Sine Wave Generator.

The procedure for the testing will involve applying a consistent load to the joint and actuating it at a controlled and consistent velocity to measure data. The data that would be measured would be the position of the system along with the force experienced by the arm-mounted sensor. This will ensure that the friction's change with respect to the motion of the system can be observed along with the change with respect to loading, angular position and angular velocity.

In order to generate an accurate model for the performance of the system, the test would need to be repeated at various angular velocities across several applied forces. This will then be translated in a model of the friction force and its variation for different flapping regimes and combinations of input variables. After a sufficiently large set of tests, it should be possible to validate this model against data collected and then use the data for further test results for other forces in the wing. The friction generated in the joint should be characterized to the point that the loading will be easily quantifiable and can be accounted for in the data for future testing of the flapping wing apparatus.

3.2. Inertia

Once the friction in the joint has been fully characterized, the next source of loading in the system to consider is the inertial loading. Contrary to conventional aircraft which utilize propellers or rotors to generate power, which operate at consistent speed or with smooth acceleration and deceleration, flapping wing systems need to rapidly reverse the direction of motion in the wing causing significant accelerations. Dragonfly wings operate at frequencies sometimes exceeding 30 Hz [4], this means that the wing's motion needs to be rapidly stopped and reversed 60 times a second. This can generate relatively large forces if the design of the wing and the system is not well optimized for mass and mass distribution.

The method for determining the amount of inertial loading is well understood for a planar motion and uses the following expressions (equations sourced from [48]).

$$T_I(t) = I_w \ddot{\theta}_w(t) \quad (4)$$

$$I_w = \int r^2 dm \quad (5)$$

where:

- T_i —The inertial loading on the wing;

- I_w —The moment of inertia of the wing;
- $\ddot{\theta}_w(t)$ —The angular acceleration of the wing;
- r —Sectional radius;
- m —Sectional mass.

If a testing apparatus has the capacity to measure the wing's acceleration in real time, the calculation of the inertial loading during operation is straightforward as all it requires as input data is prior measurement of the mass moment of inertia of the wing (I_w). This measurement would require two separate measurements to be taken, the first of which is the mass of the wing itself (m), and the second is the distance of the center of gravity of the wing from the pivot point, which is represented by r in the calculations. This could be measured with relative simplicity by finding the point along the wing's span at which the mass is balanced on either side.

With the mass and center of mass known, the mass moment of inertia can be calculated, which will give an immediate indication of the inertial loading at any defined acceleration ($\ddot{\theta}_w$). Despite these calculations being simple, it is necessary to validate them to ensure all measurements that are taken are accurate and the system is performing as expected. This is particularly important considering the masses involved (fractions of a gram).

This testing would use a similar testing apparatus as the testing for the frictional loading. The revised testing apparatus is shown in Figure 4. This testing apparatus would not feature the applied force/mass that was used to control the amount of friction in the system and instead of only actuating the arm on the mechanism, this apparatus would use a proper wing to imitate the inertial loading during flight conditions. This means the components of this system (aside from the wing) are the input (A, Figure 3) and the sensor (B). This sensor is positioned on the wing side of the pivot instead of the input side.

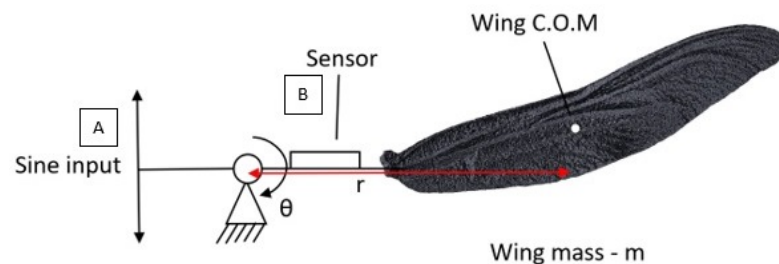


Figure 4. Inertial Testing Apparatus (wing model source: [44–46]).

The utilization of a wing causes issues around the testing of this system as the wing would generate forces due to the interactions with the air which would necessitate altering the test such that there is a way to isolate the inertial forces while effectively eliminating the aerodynamic loads.

To facilitate this, the system will be operated in a vacuum chamber. This will eliminate the aerodynamic interactions from the wing, while the frictional loading (which would be known at this point) and the inertial loading (which is what the test is measuring) will remain. It should be noted that the use of a vacuum chamber will still add difficulty to the test due to two factors. First, the efficacy of any lubricants being used can change drastically when exposed to a vacuum instead of atmosphere, which would mandate an additional test with the system in the frictional loading configuration to ensure the change in frictional loading in a vacuum is understood. The second issue is the thermal performance of a system. Whether a system is being actuated with linear actuators or rotational motors, these systems heavily rely on air cooling (through convection or forced convection), which is not feasible in a vacuum. This would mean the system would need to be tested in short bursts, allowing time to cool down between runs to prevent damage to the system.

Once these factors have been considered and mitigated, the measurement of the inertial loading is straightforward. The testing methodology requires the system to be placed into a vacuum chamber and operated at various frequencies (which would directly impact

acceleration). The forces acting on the system are measured at these various conditions. With the load acting on the system measured, the frictional load can be accounted for, and any remaining loading on the system will be predominantly (if not entirely), which is caused by the inertia of the wing's actuation.

3.3. Aerodynamics

The last and most important loading to measure and characterize is the aerodynamic loading. This is also the most complex to measure.

3.3.1. Lift and Drag Definitions

Before attempting to measure or characterize any of the aerodynamic forces in these systems, it is necessary to classify exactly what these forces represent due to different definitions existing for forces acting on an aerodynamic system.

For the flapping wing aircraft body, the primary aerodynamic forces are defined in line with Houghton et al. [49]. This definition states that the lift force is defined as the force acting upwards relative to the velocity of the aircraft, meaning it is operating perpendicular to the direction of flight or undisturbed stream.

The drag force is the force that is acting in the opposite direction to the line of flight or the same direction as the motion of the undisturbed stream. This is the force that is directly resisting the motion of the aircraft.

Both the lift and the drag are oriented relative to the velocity of the craft, meaning the direction relative to the ground changes with attitude changes in the craft; however, these are not tied to the center axis of the craft (as shown in Figure 5c). These definitions are shown in Figure 5.

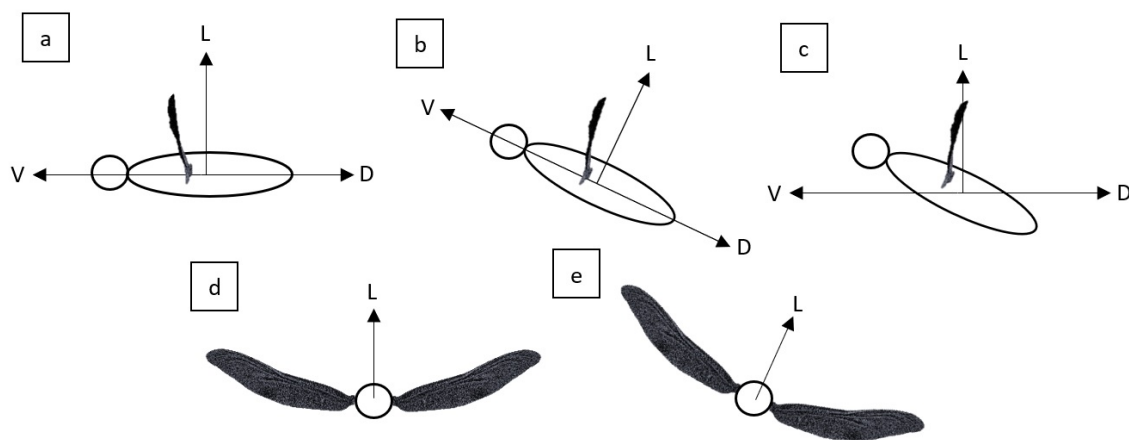


Figure 5. Lift and drag of the body with changing pitch (a–c) and roll (d,e) (wing model source: [44–46]).

For the wings themselves, their complex motion coupled with the fact that each wing moves independently and has a flapping motion, the lift and the drag are defined as per Anderson [50]. This definition states that the lift force component generated by the wing (L) is the component that is perpendicular to the airflow over the wing whether that airflow is due to body velocity (V_∞) or wing velocity (V_w) and the drag component is parallel to the airflow as is shown in Figure 6. Due to movement of the wings, this means the direction of the wings' lift and drag forces are constantly changing directions relative to the body of the craft during operation.

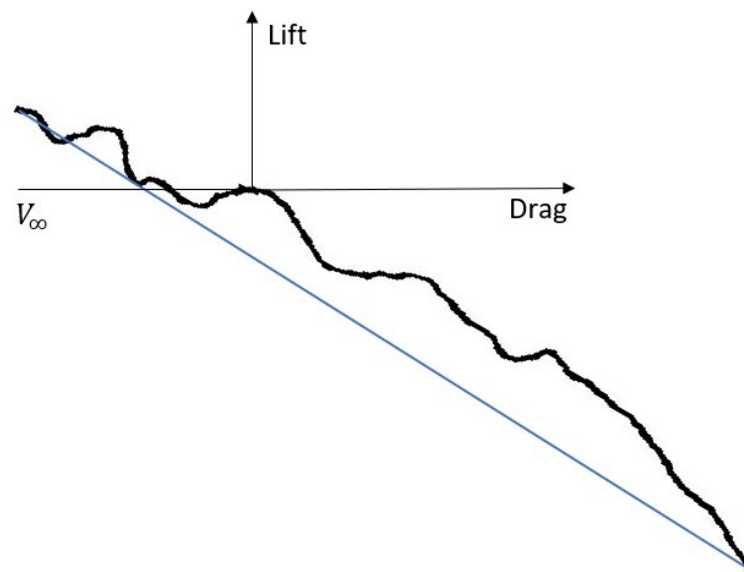


Figure 6. Wing reference lift and drag (wing profile source: [44–46]).

Ultimately, this means that the direction of wings’ lift and drag will often not align with the direction of the body’s lift and drag forces. This can be highlighted by looking at the various operational cases for the wings and the reference lift and drag forces. In the following operational cases, only strokes which are generating power will be considered. This means that in vertical operation, the upstroke which is generally not generating force is ignored; however, in horizontal operation, both the forward and back stroke are useful and therefore can be considered with the forward stroke fitting one case and the back stroke another. In addition, in cases that allow it, both horizontal and vertical flapping will be considered. Table 4 shows all of these cases that are explained in more detail below; all cells marked with an “X” are scenarios that have no operational use. The cases relative to the angle of attack are also shown diagrammatically in Figure 7 other than case 1, which does not represent the system flapping. As can be seen in this figure, there is a significant area of wing orientations that are not covered. This is because the cases covered are meant to show all feasible configurations for flapping wings and the grayed out areas represent wing orientations that would not be useful in flapping wing flight.

The cases specified in this section assume that the craft is parallel to the ground for simplicity. In actuality, systems can actuate their wings at various angles, not just horizontal or vertical, but these cases would still apply; it is only the orientation of the body lift and drag axis that would change.

In all figures in the following section, a profile of a dragonfly wing is used; this is to clearly differentiate that flapping wing profiles are differently shaped to standard airfoil wings.

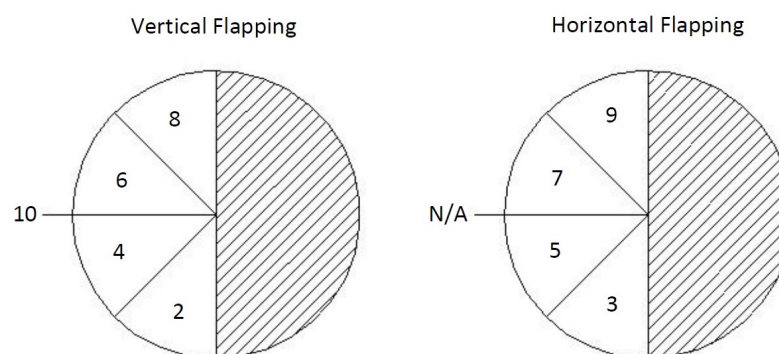


Figure 7. Wing Cases Diagram.

Table 4. Wing Operational Cases.

AOA	Flapping Direction		
	Vertical	Horizontal	None
«0	Case 2	Case 3	X
<0	Case 4	Case 5	X
0	Case 10	X	Case1
>0	Case 6	Case 7	Case 1
»0	Case 8	Case 9	Case 1

The figures are broken into two sections where applicable. These represent the two different relative velocities of the wing that cause lift production.

The first of these is the flapping motion of the wing during operation V_w . This motion can be either horizontal or vertical depending on the chosen orientation of the system, and the loading caused by this is continuously changing as the wing is constantly in motion.

The second is the air velocity over the wings caused by the motion of the craft itself V_∞ . This method of lift generation is functionally the same as the lift generation by conventional fixed wing aircraft; however, the direction and magnitude are constantly changing, as the wing’s angular positions will alter the surface area exposed to this air velocity.

In order to measure the total loading output from the wing, both of these forces need to be considered separately before being combined to yield the net force. For this reason, where applicable in all following case figures, the loading from V_w will be in the top part of the diagram, and the loading from V_∞ will be in the bottom. In cases where only one applies, only the relevant diagram will be shown.

Due to the constant motion of the wing, both forces are constantly changing in magnitude and direction during operation, so the vectors shown for L and D in the following figures are only to represent directions and are not to scale.

The first of these cases, and the simplest, is shown in Figure 8. In this case, the system is gliding, and the wings are not being actuated. This means the system is functionally operating as a fixed wing aircraft, and all lift is generated by the forward velocity of the craft, V_∞ . As Figure 8 shows, in this instance, the reference lift and drag of the wing and the reference lift and drag from the craft are both in the same direction.

$$\text{Case 1 : } L_b = L_w(V_\infty) \tag{6}$$

$$D_b = D_w(V_\infty) \tag{7}$$

This operational case would be used when the craft is conserving energy during forward flight, as it does not require significant energy expenditure to maintain, assuming the craft has sufficient height and speed to glide.

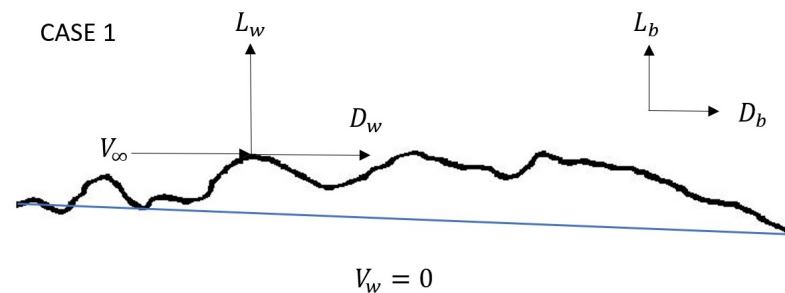


Figure 8. Wing Operation Case 1 (wing profile source: [44–46]).

The second and third operational cases are the wing operating with a significant negative angle of attack relative to the body’s direction of motion as shown in Figure 9.

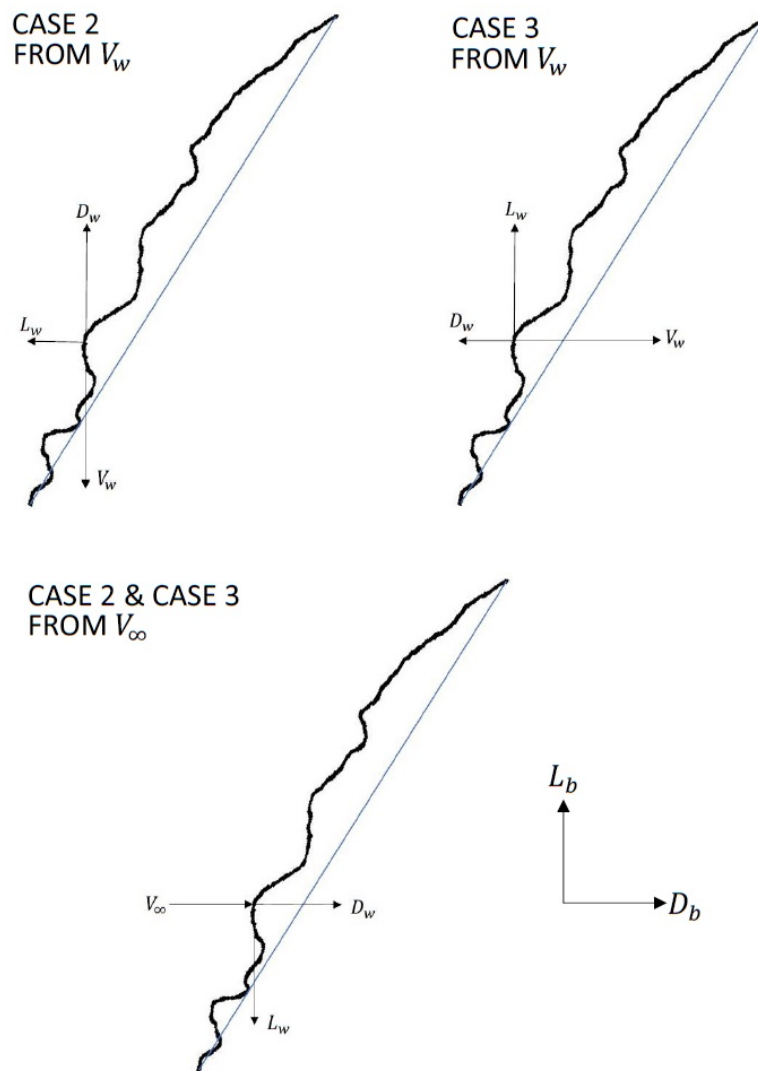


Figure 9. Wing Operation Cases 2 and 3 (wing profile source: [44–46]).

For the vertical operation of the wing (wing flaps downwards; case 2), the lift generated by the wing's motion directly counteracts the drag of the aircraft body, and the drag from the wing contributes to the lift of the body.

In horizontal operation (case 3), the wing's lift directly contributes to the lift of the body, and the wing drag counteracts the body drag.

In both cases 2 and 3, there are also aerodynamic forces that are generated from the body's motion V_∞ . The lift generated from this would be negative lift due to the wing's angle of attack but would operate in the same direction as the lift of the body, and the wing drag would be the same as the body drag.

$$\text{Case 2 : } L_b = D_w(V_w) - L_w(V_\infty) \quad (8)$$

$$D_b = -L_w(V_w) + D_w(V_\infty) \quad (9)$$

$$\text{Case 3 : } L_b = L_w(V_w) - L_w(V_\infty) \quad (10)$$

$$D_b = -D_w(V_w) + D_w(V_\infty) \quad (11)$$

The operational cases that utilize a significant negative angle of attack would be used to rapidly gain forward velocity for the body while sacrificing lift generation. The horizontal stroke (case 3) could also be used in tandem with case 9 in a hovering pattern.

The fourth and fifth operational cases would be similar to cases 2 and 3 but with a smaller negative angle of attack, as shown in Figure 10.

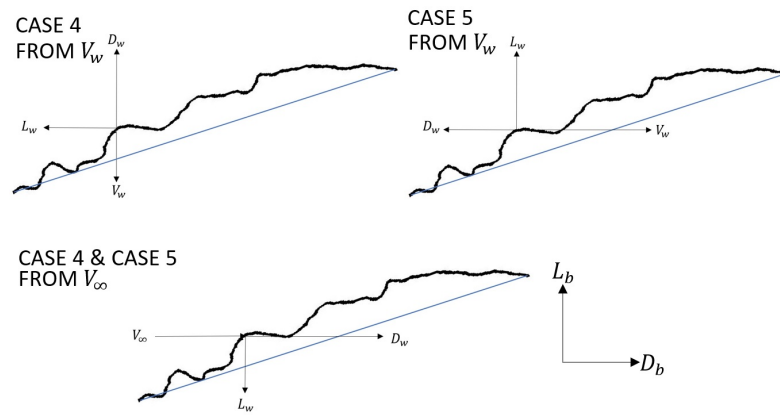


Figure 10. Wing Operation Cases 4 and 5 (wing profile source: [44–46]).

Case 4, actuating in a vertical direction, has the same characteristics as case 2. Wing lift counteracts body drag, and wing drag adds to body lift.

Case 5, operating in the horizontal direction, has the same characteristics as case 3. Wing lift is body lift, and wing drag counteracts body drag.

The loading caused by V_∞ is also the same, with wing lift being negative body lift and wing drag being body drag.

$$\text{Case 4 : } L_b = D_w(V_w) - L_w(V_\infty) \quad (12)$$

$$D_b = -L_w(V_w) + D_w(V_\infty) \quad (13)$$

$$\text{Case 5 : } L_b = L_w(V_w) - L_w(V_\infty) \quad (14)$$

$$D_b = -D_w(V_w) + D_w(V_\infty) \quad (15)$$

The differences come in the magnitudes of these forces. Using a smaller negative angle of attack means that more of the force generated by the wing's movement is being used to generate body lift and less of it is put into the body's forward motion. The negative body lift being caused by V_∞ is also lower in magnitude.

Cases 4 and 5 would be used when maintaining altitude and forward velocity or when looking to gain altitude without excessively sacrificing velocity. Case 4 can also serve as half of a hovering stroke.

The next two operational cases are when the wing is operating with a low positive angle of attack as shown in Figure 11. In case 6, when the wing is operating vertically, the lift generated by wing motion would add to the drag force on the body, against V_∞ , and the drag generated by the wing's motion would contribute to the lift of the body. In case 7, with a horizontally actuated wing, the lift caused by wing motion is the same as the body lift, whereas the drag caused by this motion contributes to body drag opposing V_∞ .

As with the other cases, there are aerodynamic forces generated by the body velocity, V_∞ . For cases 6 and 7, the lift and drag forces generated in this manner both contribute to the body lift and drag.

$$\text{Case 6 : } L_b = D_w(V_w) + L_w(V_\infty) \quad (16)$$

$$D_b = L_w(V_w) + D_w(V_\infty) \quad (17)$$

$$\text{Case 7 : } L_b = L_w(V_w) + L_w(V_\infty) \quad (18)$$

$$D_b = D_w(V_w) + D_w(V_\infty) \quad (19)$$

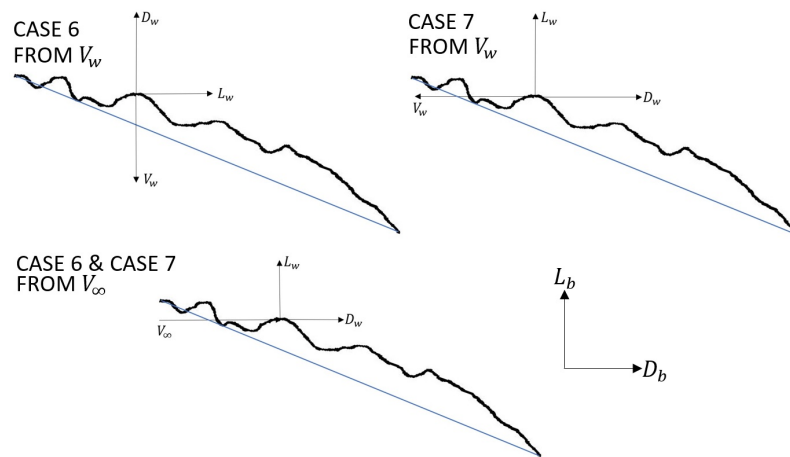


Figure 11. Wing Operation Cases 6 and 7 (wing profile source: [44–46]).

Cases 6 and 7 would be realized when there is sufficient forward velocity to maintain enough lift force to maintain altitude during forward flight as they generate lift with a small cost to the forward velocity. Case 7 specifically can also contribute to hover on horizontally actuated systems.

Cases 8 and 9 are when the wing is operating with a high positive angle of attack as shown in Figure 12. For case 8, actuating vertically, the force directions are the same as case 6. Wing lift adds to the drag of the body, and wing drag adds to body lift. For case 9, actuating horizontally, the forces align with case 7. Wing lift adds to body lift and wing drag adds to body drag.

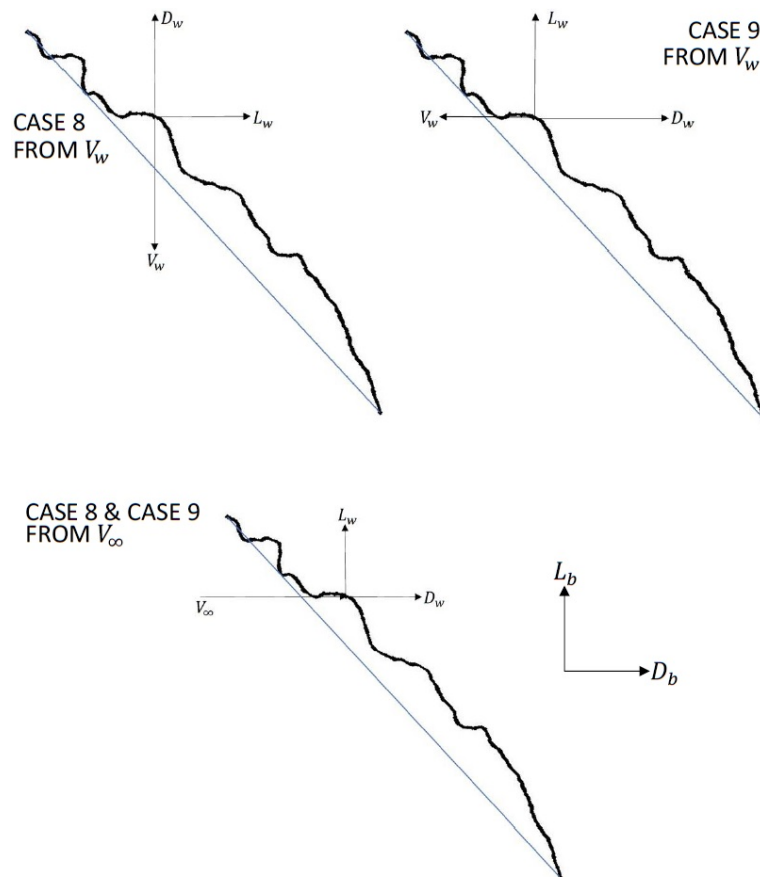


Figure 12. Wing Operation Cases 8 and 9 (wing profile source: [44–46]).

The forces caused by V_∞ in cases 8 and 9 are also the same as cases 6 and 7 with the wing lift and drag mirroring body lift and drag. The difference for cases 8 and 9 is in the distribution of these forces. Cases 8 and 9 both have significantly more force adding to the body drag with less force being applied to the body lift.

$$\text{Case 8 : } L_b = D_w(V_w) + L_w(V_\infty) \tag{20}$$

$$D_b = L_w(V_w) + D_w(V_\infty) \tag{21}$$

$$\text{Case 9 : } L_b = L_w(V_w) + L_w(V_\infty) \tag{22}$$

$$D_b = D_w(V_w) + D_w(V_\infty) \tag{23}$$

This means that the usage of cases 8 and 9 would be to arrest the forward motion of the body during operation whether this is to simply reduce speed or to move from forward flight into hovering. Case 9 can also be used during hover on a horizontal system.

The final operational case (case 10) is when the wing has effectively zero angle of attack and is actuating. This case is shown in Figure 13.

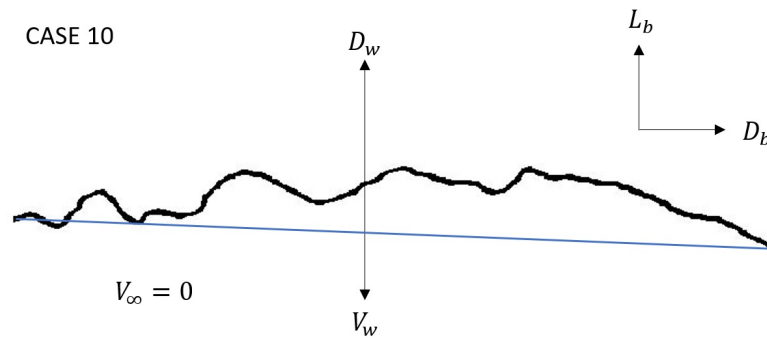


Figure 13. Wing Operation Case 10 (wing profile source: [44–46]).

In this case, there should be effectively zero wing lift generated by its motion, although any force generated in this instance would be in the same plane as the body drag. The drag generated from the wing’s motion directly contributes to the body lift. In Case 10, there should be no body velocity; as such, there should be no lift or drag forces from the wing generated by the body.

$$\text{Case 10 : } L_b = D_w(V_w) \tag{24}$$

$$D_b = 0 \tag{25}$$

Case 10 would only be used in one scenario. This is when the craft is in hover relative to the air mass and the wing actuation is being used to either maintain or increase altitude while not generating any forward motion. This case is specific to vertically actuated wings, as horizontally actuated wings would hover through using case 3/5 on one stroke and 7/9 on the return.

For simplicity, all of the usage examples for these cases consider only when all wings are operating in tandem. In order to achieve the maneuverability that is desired in a flapping wing craft, different wings would use different operational kinematics to generate unbalanced forces that would cause the desired yawing, pitching or rolling moments.

3.3.2. Aerodynamics Calculations

Flapping wing systems operate in two distinct regimes.

The first of these is the gliding regime, which corresponds to Case 1 from the previous section. For this regime, the expressions for lift and drag are the same as those that would be used for a fixed wing craft, with the flapping wing operating in a similar manner to a fixed wing as per Figure 8 in the previous section. These equations, which were adapted from Anderson [50], are below and form the basis for all the upcoming calculations.

$$L = C_L \frac{\rho V_\infty^2}{2} A \quad (26)$$

$$D = C_D \frac{\rho V_\infty^2}{2} A \quad (27)$$

In these equations:

- L is the lift;
- D is the drag;
- C_L is the lift coefficient;
- C_D is the drag coefficient;
- ρ is the air density;
- V_∞ is the air velocity;
- A is the wing area which is dependent on the wing's changing angular position (θ , β and γ).

In this regime, the lift and drag generated by the wing directly contribute to the lift and drag being experienced by the aircraft itself due to all forces being generated by the movement of the aircraft in space rather than the movement of the wings relative to the aircraft. This means that although different definitions were used for lift and drag between the aircraft and the wing, both definitions line up in this instance.

The second regime is the flapping regime. This would cover cases 2–10 from the previous section. This system is more complex to characterize, as the loading depends on the constant motion of the wings relative to each other and the body of the aircraft. For this study, the flapping wing system being discussed actuates its wings in a vertical direction (cases 2, 4, 6, 8)—this determines the direction of V_∞ induced on the wings by the motion of the body relative to the free stream.

Unlike the gliding regime, the flapping regime can operate in two distinct scenarios—either in forward motion or in hover.

When operating in forward motion (cases 2, 4, 6, 8), the same lift and drag generated in the gliding regime still apply, as there will be lift and drag forces generated by the wings from the motion of the craft itself, so Equations (26) and (27) still apply and align with the reference lift and drag of the aircraft.

In either forward or hover motion (case 10), there are also forces being generated by the actuation of the wings. These forces are where the definitions for lift and drag of the aircraft itself and the wings diverge. The motion of the wing is shown in Figure 14 and these forces are shown in Figure 15.

Firstly, considering the drag force of the wings: Due to the shape of the wings, form drag is a large component of this. As the wings are actuating vertically, the induced velocity (V_∞) is also acting vertically. This means that the drag force experienced by the wing transforms to lift force for the aircraft. In addition, due to the rotational movement of the wing, V_∞ increases across the length of the wing, maximizing near the wing tip. This means Equation (27) needs to be adjusted to consider this change in velocity, yielding Equation (28). This is shown in Figure 15 (note: the lift force would be toward or away from the page depending on wing orientation and as such is not shown).

This is the same for both forward flight and hovering flight, with the actuation of the wings being used to control the altitude of the aircraft during operation.

$$D = \int_0^R C_D \frac{\rho V_{wr}^2}{2} A_{wr} dr \quad (28)$$

In this equation:

- r is the sectional radius of the wing;
- R is the total length of the wing;
- V_{wr} and A_{wr} are the velocity and area respectively of the wing at radius r .

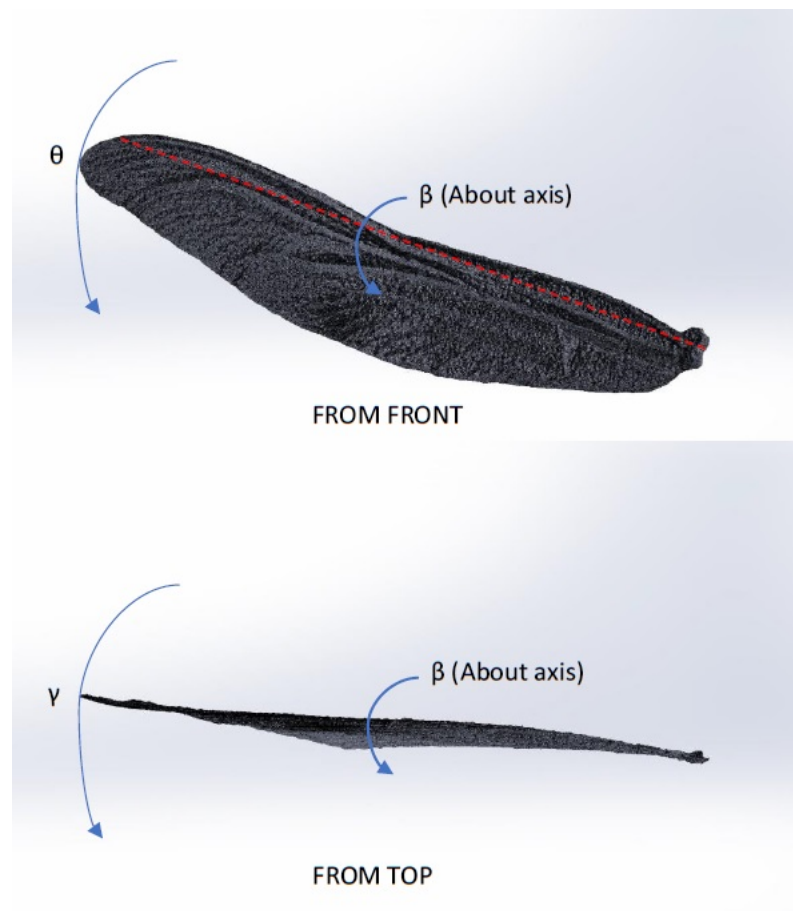


Figure 14. Motion of the Wing (wing model source: [44–46]).

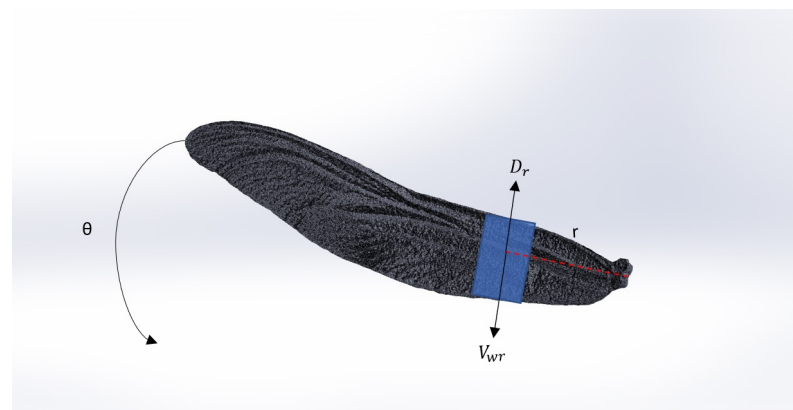


Figure 15. Forces from wing motion (wing model source: [44–46]).

As for the wing lift force, the application of it differs depending on whether the craft is in forward motion or if it is hovering. In either instance, the lift force requires a similar adjustment from Equation (26) to the drag, as shown in Equation (29).

$$L = \int_0^R C_L \frac{\rho V_{wr}^2}{2} A_{wr} dr \quad (29)$$

When the craft is in forward motion, the lift force of the wing (perpendicular to V_∞) would either augment or counteract the drag force of the aircraft. This means the defined lift force of the wing generated through actuation is contributing to the horizontal motion of the aircraft.

In hovering flight, the net horizontal force on the aircraft should be zero or close to zero. However, during actuation of the wings to generate the form drag required for hover, there is likely to be a parasitic wing lift force generated which would need to be counteracted by other wings on the craft to keep the overall horizontal force to zero.

In order to use the expressions to calculate the forces being generated by the wing, it would require knowing the coefficients of lift and drag of the wing (C_L and C_D respectively) at a variety of angles relative to the wing velocity (V_w). This would require significant wind tunnel testing to characterize the wings.

Experimentation to determine the aerodynamic loading would use the same apparatus as that used in the inertial load testing. The angle of attack and angle of sweep could be set in the operation of this system or they could be varied and controlled. The angular velocity could either be measured and controlled through actuation with fine levels of control and calculation or through high-speed video.

Testing for aerodynamic loading would be in three discrete sections. The first of these would require the vacuum chamber as per the inertial loading but with the pressure being added to the vessel in controlled increments to observe the changes in aerodynamic loading across various pressures of air, which would give a good characterisation of the forces across a variety of scenarios. If all loading on the system is measured during these tests, the frictional and inertial loads, which are known, can be accounted for, and all that would remain is the aerodynamic loading caused by the motion of the wing.

The second section would require a wind tunnel. The forces exerted by the wing would need to be measured across a variety of air speeds and angles of attack and sweep. The data measured from this should not have any inertial or frictional loading as the system does not need to be actuating the wing for this test. Once enough data are taken from this testing, the performance of the wing caused by the forward motion of the craft can be well characterized, modeled and understood.

The last aspect of testing that would need to be completed to finish characterizing the aerodynamic loading would be a combination of the previous two tests. This would mean the wing would be actuated while experiencing air rushing over it in a similar fashion to what the craft's forward motion would generate. With the inertial loading, frictional loading and aerodynamic loading generated from both actuation and wind speed all being known at this stage, it should be achievable to characterize all loads experienced by the system during operation and fully model the characteristics of the wings for all regimes.

3.3.3. Blade Element Method

As mentioned in the previous section, the angular wing motion used in a flapping wing system causes the velocity of the wings to vary across the span of the wing.

This means the conventional equations to calculate lift and drag would not give accurate results. There are existing methods to determine the performance of a wing with rotary motion, in particular blade element analysis. It is used for aircraft elements such as propellers or rotors and it could be feasible to assume the flapping wing is operating as a rotor and utilize these existing equations to determine the performance.

However, the motion of a flapping wing is more complex, with constantly changing kinematics and more degrees of freedom than a conventional rotor would experience.

In order to fully break down the performance of a flapping wing system, breaking the wings down into sectional elements and calculating each of these elements for every time-step of the wing's operation is another viable method to determine the performance.

For this, the adapted equations for wing lift and drag for the previous section are recalled as these will form the basis for these calculations.

$$L(t) = \int_0^R C_L \frac{\rho V(t)^2}{2} A(t) dr \quad (30)$$

$$D(t) = \int_0^R C_D \frac{\rho V(t)^2}{2} A(t) dr \quad (31)$$

The lift and drag generated by the wing are broken into two aspects, which depend on the source of the velocity V . The first is forces generated by the wing's flapping motion (V_w), and the forces generated by the body's forward velocity (V_∞).

The lift and drag generated by the wing's motion will be considered first as the calculations are the same for both horizontal and vertical flapping wing systems with only the directions of wing lift and drag relative to the body differing.

The variables in Equations (30) and (31) need to be considered and defined with respect to the movement of the wing as a whole along with the individual elements.

Firstly, C_L and C_D . These variables are both only defined through experimentation, so they need to be measured and determined in advance. These will vary depending on the profile of wing used in the flapping wing system, and they will also vary based on the position of the wing relative to the airflow, so extensive characterization of the wing is necessary.

Density ρ varies with altitude and can be taken from existing data.

$V_{wr}(t)$ is the first of the variables that changes across the span of the wing and changes with time. Thus,

$$V_{wr}(t) = \dot{\theta}(t)r \quad (32)$$

where r is the radius of the section being analyzed, and $\dot{\theta}(t)$ is the instantaneous angular velocity of the wing.

The last variable, $A(t)$ is replaced by $A_{wr}(t)$ which represents the area of the wing section that is exposed to the wing velocity. This variable is constantly changing depending on the angular position in the flapping (θ), sweep (γ) and pitching (β) axes. The relation of these variables depends on the design of the wing along with the specific kinematics of the wing; therefore,

$$A_{wr}(t) = f[\theta(t), \gamma(t), \beta(t)] \quad (33)$$

When these variables are all defined, the lift and drag forces generated by the wing's movement can be determined.

The next consideration is the lift and drag generated by the body's movement V_∞ .

This still uses similar equations to Equations (30) and (31); however, the velocity used in this instance (V_∞) is constant across the span of the wing, and as such, it is not necessary to break the wing down into elements to determine the resultant lift.

The remaining variables remain the same other than $A(t)$, which is instead represented by $A_\infty(t)$. This variable is the area of the entire wing face that is exposed to the airflow from the body movement, and it is still determined by the wing's angular positions, such that:

$$A_\infty(t) = f[\theta(t), \gamma(t), \beta(t)] \quad (34)$$

Determining all of these variables would allow the lift and drag forces generated by the body velocity to be determined.

To finalize this, the forces generated by body movement and wing movement can be combined to yield the overall forces experienced by the body generated by the wing. This is where vertically actuated wings and horizontally actuated wings differ.

For a vertically actuated wing, the determination of these forces uses the following.

$$|L_b(t)| = \left[\int_0^R C_D \frac{\rho V_{wr}(t)^2}{2} A_{wr}(t) dr \right] \pm C_L \frac{\rho V_\infty(t)^2}{2} A_\infty(t) \quad (35)$$

$$|D_b(t)| = \left[\int_0^R C_L \frac{\rho V_{wr}(t)^2}{2} A_{wr}(t) dr \right] \pm C_D \frac{\rho V_\infty(t)^2}{2} A_\infty(t) \quad (36)$$

Whereas for a horizontally actuated wing, the equations are below.

$$|L_b(t)| = \left[\int_0^R C_L \frac{\rho V_{wr}(t)^2}{2} A_{wr}(t) dr \right] \pm C_L \frac{\rho V_\infty(t)^2}{2} A_\infty(t) \quad (37)$$

$$|D_b(t)| = \left[\int_0^R C_D \frac{\rho V_{wr}(t)^2}{2} A_{wr}(t) dr \right] \pm C_D \frac{\rho V_\infty(t)^2}{2} A_\infty(t) \quad (38)$$

In both sets of equations:

- L_b and D_b represent the absolute values for lift and drag in the body frame;
- C_L and C_D represent the coefficients of lift and drag, respectively;
- ρ is air density;
- V_{wr} is the linear velocity of the section of the wing at radius r ;
- A_{wr} is the sectional area at radius r exposed to the airflow generated by V_{wr} ;
- V_∞ is the airflow on the wing caused by the body velocity;
- A_∞ is the area of the wing exposed to the airflow generated by V_∞ .

In these equations, the plus-minus is used because the lift and drag forces generated by wing movement and body movement can either augment or detract from one another depending on the wing orientation, as shown in Section 3.3.1. This section also shows why lift and drag expressions are combined for Equations (35) and (36).

If parameters of the wing itself are well characterized, these equations are another method to determine the aerodynamic loading during operation.

To test the aerodynamic performance of the wings, a similar method to that of Benedict et al. [40,41] will be utilized. This will entail operating the wing in a normal environment with the same kinematics as the inertial testing regime and collecting data. From these data, the known measurements from the inertial and frictional testing can be accounted for, which leaves predominantly aerodynamic loading in the data. This allows the system's performance regarding the aerodynamic, inertial and frictional loading to be determined.

3.4. Elasticity and Hysteresis

Due to the wings on a flapping wing system needing to be as light as possible to replicate nature, there is a potential for the wings to flex during operation which can have a significant impact on the forces and a lesser but measurable impact on the losses during actuation. This flexing would potentially manifest itself as a phase shift on the aerodynamic forces being produced by the wing.

At present, the elasticity and hysteresis of the wing itself is not within the scope of this work. However, in future developments, the measurements to characterize the wing elasticity will be performed in a vacuum by varying the wing actuation speed and measuring the deformation of the wing during operation. We anticipate that this measurement will likely be taken using high-speed vision complementing the position/motion/force measurements, and when forces are compared to the input signal, it should demonstrate a phase delay between the input to the base of the wing and the tip of the wing caused by the wing flex.

3.5. Previous Testing

Initial testing for flapping wing systems was completed using a small force sensing resistor built into a simple flapping wing mechanism [30]. This testing was able to yield results but demonstrated that there was a need for further analysis and understanding of what was being measured, along with optimization of a sensor system suitable for these systems.

It also showed that a sensor measuring the overall performance of the system could be easily dominated by vibrations, inertial or other parasitic forces which impaired the ability to accurately measure the system's performance. This highlighted the need to determine a testing regime that could isolate the major forces to measure, which is the aim of this paper.

4. Discussion

Due to their complexity and the design parameters around them, measuring the performance characteristics of a flapping wing system is challenging. As with most complex mechanical systems, there is no simple “one size fits all” solution to these measurements, and instead, it will require specific equipment to measure various aspects of the system.

With the initial analysis of existing flapping wing test apparatus, it was evident that there was no clear capability to measure the full performance of a flapping wing system from end to end. As such, a testing methodology was designed to rectify this.

The testing methodology laid out in this paper demonstrates a clear way forward in these measurements, and the completion of this testing regime should yield the performance of a flapping wing system in reasonable detail with only minor losses yet to be considered.

This methodology is capable of filling the gaps in the existing works around flapping wing instrumentation, as it is capable of providing detail on not only how much loading is occurring in a system but also what form of loading it is. If the input torque/force is known, this information could also be used to determine the efficiency of a flapping wing system.

In addition, if the testing methodology outlined in this paper is completed, it could be used in flight measurement on a system that had been characterized, modeled and understood previously. This would mean the potential for developing and testing a system to the point that it is fully understood before flight testing.

The only major challenge that remains in the development of this instrumentation is the selection of an appropriate sensor to measure the forces as required. This requires a sensor that is accurate enough to measure the relatively small forces generated by the system particularly in the testing around the frictional and inertial loading. However, consideration also must be given as to whether this sensor is capable of being used in flight.

If an appropriate sensor can be chosen, it should be feasible to use the testing configuration and methodology described in this paper to characterize the performance of almost any flapping wing system that may be developed.

5. Conclusions

This paper has laid out the major forces and losses that need to be considered in the testing and development of a flapping wing style system. This paper integrates a systematic analysis of all types of forces that occur in a flapping wing system as a basis for well-designed and fully functional instrumentation for the testing and operation of these systems. This includes, in premiere, a systematic analysis of all cases that can create either useful or parasitic aerodynamic loads.

The information within this paper demonstrates the areas of focus for any flapping wing system in order to increase useful forces and decrease parasitic forces in order to extract as much useful energy as possible during operation. It also provides a guide as to how these forces can be measured to allow any existing or new system to optimize the forces mentioned herein.

The next step in this work is to implement the testing methodologies outlined in this paper on a system analogous to a flight capable flapping wing craft.

This testing will serve two major purposes. The first of these is to support the development of a simulation model of the system. This requires extensive testing, but once the model is fully defined and validated, it would enable the system’s performance in a variety of conditions to be accurately estimated without the need for extensive testing.

The second purpose is that it could lead to in-flight instrumentation for flapping wing systems, which would be an essential feature of any flapping wing system that aims to replicate the performance of natural flapping wing flyers with their comprehensive sensor installation.

The research presented in this paper is a key step and a condition in the quest for the ultimate goal of this work to create a fully functional and accurate suite of instrumentation for flapping wing systems.

Author Contributions: Conceptualization, A.T.L., R.M.M. and J.S.C.; Investigation, A.T.L.; Methodology, A.T.L. and R.M.M.; Project Administration, R.M.M. and J.S.C.; Supervision, R.M.M. and J.S.C.; Visualization, A.T.L.; Writing—Original Draft, A.T.L.; Writing—Review and Editing, A.T.L., R.M.M. and T.O. All authors have read and agreed to the published version of the manuscript.

Funding: This research received no external funding.

Institutional Review Board Statement: Not applicable.

Informed Consent Statement: Not applicable.

Data Availability Statement: Not applicable.

Acknowledgments: This research work was accomplished with the support of the Australian Government Research Training Program (RTP). The wing models used for the various figures in Section 3.3.1 were all adapted from the works of Nasim Chitsaz.

Conflicts of Interest: The authors declare no conflict of interest. The funders had no role in the design of the study; in the collection, analyses, or interpretation of data; in the writing of the manuscript, or in the decision to publish the results.

References

- Liu, Z.; Moschetta, J. Rotary vs. flapping wing nano air vehicles: Comparing hovering power. In Proceedings of the European Micro Aerial Vehicle Conference, Delft, The Netherlands, 14–17 September 2009; pp. 21–27.
- Michelson, R.; Reece, S. Update on flapping wing micro air vehicle research—ongoing work to develop a flapping wing, crawling entomopter. In Proceedings of the 13th Bristol International RPV/UAV Systems Conference, Bristol, England, 30 March–1 April 1998; Volume 30, pp. 30–31.
- Boon, M.; Drijfhout, A.; Tesfamichael, S. Comparison of fixed-wing and multi-rotor UAV for environmental mapping applications: A case study. *Int. Arch. Photogramm. Remote Sens. Spat. Inf. Sci.* **2017**, *42*, 47. [[CrossRef](#)]
- Rüppell, G. Kinematic analysis of symmetrical flight manoeuvres of odonata. *J. Exp. Biol.* **1989**, *144*, 13–42. [[CrossRef](#)]
- Wakeling, J.; Ellington, C. Dragonfly flight. I. Gliding flight and steady-state aerodynamic forces. *J. Exp. Biol.* **1997**, *200*, 543–556. [[CrossRef](#)] [[PubMed](#)]
- Azuma, A.; Watanabe, T. Flight performance of a dragonfly. *J. Exp. Biol.* **1988**, *137*, 221–252. [[CrossRef](#)]
- May, M. A critical overview of progress in studies of migration of dragonflies (odonata:anisoptera), with emphasis on North America. *J. Insect Conserv.* **2013**, *17*, 1–15. [[CrossRef](#)]
- Alexander, D. Wind tunnel studies of turns by flying dragonflies. *J. Exp. Biol.* **1986**, *122*, 81–98. [[CrossRef](#)]
- Necker, R. Observations on the function of a slowly-adapting mechanoreceptor associated with filoplumes in the feathered skin of pigeons. *J. Comp. Physiol. A* **1985**, *156*, 391–394. [[CrossRef](#)]
- Hörster, W. Vibrational sensitivity of the wing of the pigeon (*Columba livia*)—A study using heart rate conditioning. *J. Comp. Physiol. A* **1990**, *167*, 545–549. [[CrossRef](#)]
- Hörster, W. Histological and electrophysiological investigations on the vibration-sensitive receptors (Herbst corpuscles) in the wing of the pigeon (*Columba livia*). *J. Comp. Physiol. A* **1990**, *166*, 663–673. [[CrossRef](#)]
- Brown, R.E.; Fedde, M.R. Airflow sensors in the avian wing. *J. Exp. Biol.* **1993**, *179*, 13–30. [[CrossRef](#)]
- Yan, J.; Wood, R.J.; Avadhanula, S.; Sitti, M.; Fearing, R.S. Towards flapping control for a micromechanical flying insect. In Proceedings of the 2001 ICRA—IEEE International Conference on Robotics and Automation (Cat. No.01CH37164), Seoul, Korea (South), 21–26 May 2001; Volume 4, pp. 3901–3908.
- Avadhanula, S.; Wood, R.; Steltz, E.; Yan, J.; Fearing, R. Lift force improvements for the micromechanical flying insect. In Proceedings of the 2003 IEEE/RSJ International Conference on Intelligent Robots and Systems (IROS 2003) (Cat. No.03CH37453), Las Vegas, NV, USA, 27–31 October 2003; Volume 2, pp. 1350–1356.
- Yan, J.; Fearing, R.S. Wing force map characterization and simulation for the micromechanical flying insect. In Proceedings of the 2003 IEEE/RSJ International Conference on Intelligent Robots and Systems (IROS 2003) (Cat. No.03CH37453), Las Vegas, NV, USA, 27–31 October 2003; Volume 2, pp. 1343–1349.
- Syaifuddin, M.; Park, H.C.; Goo, N.S. Design and evaluation of a LIPCA-actuated flapping device. *Smart Mater. Struct.* **2006**, *15*, 1225. [[CrossRef](#)]
- Wood, R. Design, fabrication and analysis of a 3DOF, 3cm flapping-wing MAV. In Proceedings of the 2007 IEEE/RSJ International Conference on Intelligent Robots and Systems, San Diego, CA, USA, 29 October–2 November 2007; pp. 1576–1581.
- Conn, A.T.; Burgess, S.C.; Ling, C.S. Design of a parallel crank-rocker flapping mechanism for insect-inspired micro air vehicles. *Proc. Inst. Mech. Eng. Part C J. Mech. Eng. Sci.* **2007**, *221*, 1211–1222. [[CrossRef](#)]
- Conn, A.T.; Burgess, S.C.; Ling, C.S.; Vaidyanathan, R. The design optimisation of an insect-inspired micro air vehicle. *Int. J. Des. Nat. Ecodyn.* **2008**, *3*, 12–27. [[CrossRef](#)] [[PubMed](#)]
- Nguyen, V.; Syaifuddin, M.; Park, H.; Byun, D.; Goo, N.; Yoon, K. Characteristics of an insect-mimicking flapping system actuated by a unimorph piezoceramic actuator. *J. Intell. Mater. Syst. Struct.* **2008**, *19*, 1185–1193. [[CrossRef](#)]

21. Bejgerowski, W.; Ananthanarayanan, A.; Mueller, D.; Gupta, S.K. Integrated product and process design for a flapping wing drive mechanism. *J. Mech. Des.* **2009**, *131*, 061006. [[CrossRef](#)]
22. Mueller, D.; Bruck, H.; Gupta, S. Measurement of thrust and lift forces associated with drag of compliant flapping wing for micro air vehicles using a new test stand design. *Exp. Mech.* **2010**, *50*, 725–735. [[CrossRef](#)]
23. Nguyen, Q.; Park, H.; Goo, N.; Byun, D. Characteristics of a beetle's free flight and a flapping-wing system that mimics beetle flight. *J. Bionic Eng.* **2010**, *7*, 77–86. [[CrossRef](#)]
24. George, R.; Colton, M.; Mattson, C.; Thomson, S. A differentially driven flapping wing mechanism for force analysis and trajectory optimization. *Int. J. Micro Air Veh.* **2012**, *4*, 31–49. [[CrossRef](#)]
25. Nguyen, Q.; Chan, W.; Debiasi, M. Hybrid design and performance tests of a hovering insect-inspired flapping-wing micro aerial vehicle. *J. Bionic Eng.* **2016**, *13*, 235–248. [[CrossRef](#)]
26. Nguyen, T.; Phan, H.; Au, T.; Park, H. Experimental study on thrust and power of flapping-wing system based on rack-pinion mechanism. *Bioinspir. Biomim.* **2016**, *11*, 046001. [[CrossRef](#)]
27. Phan, H.; Kang, T.; Park, H. Design and stable flight of a 21 g insect-like tailless flapping wing micro air vehicle with angular rates feedback control. *Bioinspir. Biomim.* **2017**, *12*, 036006. [[CrossRef](#)] [[PubMed](#)]
28. Nguyen, Q.V.; Chan, W.L. Development and flight performance of a biologically-inspired tailless flapping-wing micro air vehicle with wing stroke plane modulation. *Bioinspir. Biomim.* **2018**, *14*, 016015. [[CrossRef](#)] [[PubMed](#)]
29. Gong, D.; Lee, D.; Shin, S.; Kim, S. String-based flapping mechanism and modularized trailing edge control system for insect-type FWMAV. *Int. J. Micro Air Veh.* **2019**, *11*, 1756829319842547. [[CrossRef](#)]
30. Lefik, A.T.; Chahl, J.S.; Marian, R. Concept instrumentation for flapping wing UAVs and MAVs. In *AIAC 2018: 18th Australian International Aerospace Congress HUMS-11th Defence Science and Technology (DST) International Conference on Health and Usage Monitoring (HUMS 2019): ISSFD-27th International Symposium on Space Flight Dynamics (ISSFD)*; Royal Aeronautical Society: Crows Nest, Australia, 2019; p. 406.
31. Deng, H.; Xiao, S.; Huang, B.; Yang, L.; Xiang, X.; Ding, X. Design optimization and experimental study of a novel mechanism for a hover-able bionic flapping-wing micro air vehicle. *Bioinspir. Biomim.* **2020**, *16*, 026005. [[CrossRef](#)] [[PubMed](#)]
32. Lane, P.; Throneberry, G.; Fernandez, I.; Hassanalian, M.; Vasconcellos, R.; Abdelkefi, A. Towards Bio-Inspiration, Development, and Manufacturing of a Flapping-Wing Micro Air Vehicle. *Drones* **2020**, *4*, 39. [[CrossRef](#)]
33. Phan, H.V.; Aurecianus, S.; Au, T.K.L.; Kang, T.; Park, H.C. Towards the long-endurance flight of an insect-inspired, tailless, two-winged, flapping-wing flying robot. *IEEE Robot. Automat. Lett.* **2020**, *5*, 5059–5066. [[CrossRef](#)]
34. Tu, Z.; Fei, F.; Zhang, J.; Deng, X. An at-scale tailless flapping-wing hummingbird robot. I. Design, optimization, and experimental validation. *IEEE Trans. Robot.* **2020**, *5*, 1511–1525. [[CrossRef](#)]
35. Yang, L.; Hsu, C.; Ho, J.; Feng, C. Flapping wings with PVDF sensors to modify the aerodynamic forces of a micro aerial vehicle. *Sens. Actuators A Phys.* **2007**, *139*, 95–103. [[CrossRef](#)]
36. Yang, W.; Wang, L.; Song, B. Dove: A biomimetic flapping-wing micro air vehicle. *Int. J. Micro Air Veh.* **2018**, *10*, 70–84. [[CrossRef](#)]
37. Nian, P.; Song, B.; Xuan, J.; Yang, W.; Dong, Y. A wind tunnel experimental study on the flexible flapping wing with an attached airfoil to the root. *IEEE Access* **2019**, *7*, 47891–47903. [[CrossRef](#)]
38. Truong, N.T.; Phan, H.V.; Park, H.C. Design and demonstration of a bio-inspired flapping-wing-assisted jumping robot. *Bioinspir. Biomim.* **2019**, *14*, 036010. [[CrossRef](#)] [[PubMed](#)]
39. Liu, C.; Li, P.; Song, F.; Stamhuis, E.J.; Sun, J. Design optimization and wind tunnel investigation of a flapping system based on the flapping wing trajectories of a beetle's hindwings. *Comput. Biol. Med.* **2022**, *140*, 105085. [[CrossRef](#)] [[PubMed](#)]
40. Benedict, M.; Coleman, D.; Mayo, D.B.; Chopra, I. Experiments on rigid wing undergoing hover-capable flapping kinematics at micro-air-vehicle-scale Reynolds numbers. *AIAA J.* **2016**, *54*, 1145–1157. [[CrossRef](#)]
41. Seshadri, P.; Benedict, M.; Chopra, I. Understanding micro air vehicle flapping-wing aerodynamics using force and flowfield measurements. *J. Aircr.* **2013**, *50*, 1070–1087. [[CrossRef](#)]
42. Conn, A.; Burgess, S.; Hyde, R.; Ling, C.S. From natural flyers to the mechanical realization of a flapping wing micro air vehicle. In *Proceedings of the 2006 IEEE International Conference on Robotics and Biomimetics*, Kunming, China, 17–20 December 2006; pp. 439–444.
43. Zárate, J.; Witte, H. Design and Control of a Flapping Wing System Test Bench. In *International Conference on Robotics in Alpe-Adria Danube Region*; Springer: Cham, Switzerland, 2019; pp. 34–42.
44. Chitsaz, N.; Marian, R.; Chahl, J. Experimental method for 3D reconstruction of Odonata wings (methodology and dataset). *PLoS ONE* **2020**, *15*, e0232193. [[CrossRef](#)] [[PubMed](#)]
45. Chitsaz, N.; Marian, R.; Chitsaz, A.; Chahl, J.S. Parametric and Statistical Study of the Wing Geometry of 75 Species of Odonata. *Appl. Sci.* **2020**, *10*, 5389. [[CrossRef](#)]
46. Chitsaz, N.; Siddiqui, K.; Marian, R.; Chahl, J. An experimental study of the aerodynamics of micro corrugated wings at low Reynolds number. *Exp. Therm. Fluid Sci.* **2021**, *121*, 110286. [[CrossRef](#)]
47. Artobolevsky, I.I. *Mechanisms in Modern Engineering Design, Volume II: Lever Mechanisms*; MIR Publishers: Moscow, Russia, 1976.
48. Giancoli, D.C. *Physics for Scientists & Engineers with Modern Physics*; Pearson: London, UK, 2014.
49. Houghton, E.L.; Carpenter, P.W. *Aerodynamics for Engineering Students*; Elsevier: Amsterdam, The Netherlands, 2003.
50. Anderson, J.D. *Fundamentals of Aerodynamics*; McGraw Hill: New York, NY, USA, 1991.